Small non-significant increments in single-subject voxel-wise statistics lead to significant group level improvements with multiband for task-based fMRI

Ritu Bhandari[1], Valeria Gazzola[1,2+] and Christian Keysers[1,2+#]

1. Netherlands Institute for Neuroscience, KNAW, Amsterdam, The Netherlands
2. Department of Psychology, University of Amsterdam, The Netherlands

+ Equally contributing last authors.

Correspondence can be directed to c.keysers@nin.knaw.nl

Abstract

Most previous studies that assessed task correlated BOLD for quantifying performance of Multiband (MB) acceleration, concluded their findings using summary statistics such as mean t-values within a region of interest (ROI) at the single-subject-level followed by post-hoc comparisons to identify the winning sequences. However, there are no studies so far that directly contrast sequences with and without MB acceleration to see if there is any benefit on the single-subject voxel-wise statistics. This is the first study that directly compares voxel-wise statistics between different sequences with varying acceleration achieved using MB to show that for task based studies, there is no advantage of MB in improving single subject level statistics. However, going from no acceleration to MB factor 4 we see small non-significant improvements in individual subject statistics, which potentially leads to improvements seen at group level with higher acceleration.

Keywords

Simultaneous multi slice, within-subject ANOVA, single-subject statistics, z-transformation

1. Introduction

Functional magnetic resonance imaging (fMRI) is increasingly used as a non-invasive pre-surgical tool for planning function-preserving neurosurgeries for epilepsy and brain tumor patients (Lindquist & Mejia, 2015; Nadkarni et al., 2014; Ni, Wang, Yu, Wu, & Wang, 2019; Wengenroth et al., 2011). Given the extreme importance of the outcome from such examinations, it is critical to use a scanning sequence that would result in the most robust estimations of activation in different brain regions. Multiband (MB) accelerated scanning that allows the acquisition of magnetic resonance imaging (MRI) signals from more than one spatial coordinate at a time has been tested in over 40 studies with resting state and task-based fMRI (for a detailed overview see Bhandari et al., 2019). The advantages offered by this acquisition scheme that affords higher sampling rate have been shown in many resting state studies (Feinberg et al., 2010; Griffanti et al., 2014; Koopmans, Boyacioğlu, Barth, & Norris, 2012; Preibisch, Castrillón G., Bührer, & Riedl, 2015). Several task based fMRI studies also show comparable or better results for MB accelerated sequences (Chen et al., 2015; Demetriou et al., 2018; Moeller et al., 2010; Sahib et al., 2018; Todd et al., 2017). In our recent study we analysed task based fMRI data acquired with multiple sequences with different MB+SENSE acceleration factors and showed that at group-level, sequences with MB acceleration perform better in terms of voxel-wise t-values (Bhandari et al., 2019). This was one of only two studies (Boyacioğlu, Schulz, Koopmans, Barth, & Norris, 2015) that quantified and compared the effects of MB acceleration on a group level, voxel-wise statistic. Most other studies that assessed task correlated BOLD for quantifying performance of MB acceleration, concluded their findings using summary statistics such as mean t-values within a region of interest (ROI) at the single subject level (Kiss, Hermann, Vidnyánszky, & Gál, 2018; McDowell & Carmichael, 2018; Sahib et al., 2018, 2016; Todd et al., 2016). However, there are no studies so far that directly contrast sequences with and without MB acceleration, in the same statistical model, to see if there is any benefit on single subject voxel-wise statistics.

Comparing within-subject voxel-wise statics is important to better understand the effects of MB acceleration on task based fMRI as it presents a complete picture of the of the advantages and disadvantages of the sequence throughout the brain. ROI approach on the other hand while has the advantage of lower chances of type I and II errors, may be influenced by factors such as ROI selection strategy, size of the ROI as well as within-ROI averaging of the signal, and may lead to higher/lower t-values due to a subset of voxels in the ROI. Moreover, direct voxel-wise comparison also allows cluster level corrections to ensure the consistency of the effect over a broader network. In this work, we therefore computed within-subject ANOVA that would directly contrast the statistics between sequences to reveal if there is a consistent improvement in the ability to detect the task network with increased acceleration. Finally, as opposed to the post-hoc testing using the ROI approach, this approach presents direct evidence for the impact of MB on single-subject statistics.

One important thing to consider while directly comparing the subject level statics coming from different sequences and therefore different sample size within a model is that the subject-level t-values and the critical t-values are estimated using the degrees of freedom that are dependent on the number of samples. Therefore in absence of any standardization (e.g. Z-transformation), the results may be biased towards sequences that have more samples. This complicates the interpretation of the actual benefits of MB at the single subject level.

The contrast or the beta maps are not affected by the sampling rate. However, these cannot be used while comparing MB acceleration as one of the side effects of accelerated sampling is the loss in grey-white

contrast in the functional images (Bhandari et al., 2019). This paired to the default global normalization in SPM, which is necessary to homogenize the data coming from different subjects and groups, would result in a spurious difference across acquisition schemes due to different grey-white contrast that results from the shorter acquisition time, which in turn leads to less T1 recovery. One way to directly compare the data coming from two sequences, which result in different total sample numbers, is to use z-statistics. Given the known degrees of freedom and the t-value per voxel, one can calculate p-values and then convert them to z-values (from here on referred to as t-p-z) to make the result normally distributed. While the t-statics can change with the degrees of freedom, the t-p-z transformation allows us to look at a transformed p value (z-distribution), which is not biased by the degrees of freedom. This allows direct comparison of data between sequences within the same statistical model. Alternatively, one can look at the "effect-size" z-values, which requires the normalization of the t-values by dividing them by the square root of the degrees of freedom (from here on referred to as es-z). The es-z transformation normalizes the t-values for the difference in the degrees of freedom, thereby allowing direct comparison.

To visualize the impact of higher sampling and the effect of different z-transformations, we drew a vector of 1000 numbers from a mu=0.2 and s=1 random normal distribution to simulate an effect size of d=0.2. The p and t value of a t-test comparing the first n of these numbers against zero, varying n from 50 to 1000 were computed. Both t-p-z and es-z transformations were performed. Figure 1 presents the plots of t, p, t-p-z and es-z and shows that while t, p and t-p-z shows the expected linear (or slightly curvilinear) increase with the increasing data points, the es-z transformation shows a more or less constant values with increasing data points. This is because the es-z transformation reflects the magnitude of BOLD change between conditions and is dependent on the task SNR, which is not expected to change with sampling rate as long as the quality of measurements in terms of the noise remains the same. While this simulation confirms that increasing the statistical power should lead to better t and p estimations, it does not take into account (a) the increased noise and (b) the increased temporal auto-correlation with higher sampling rate. The results of the direct comparison of different MB sequences will thus show if the advantages of higher sampling surpass the negative effects of the increased noise and noise correlation.

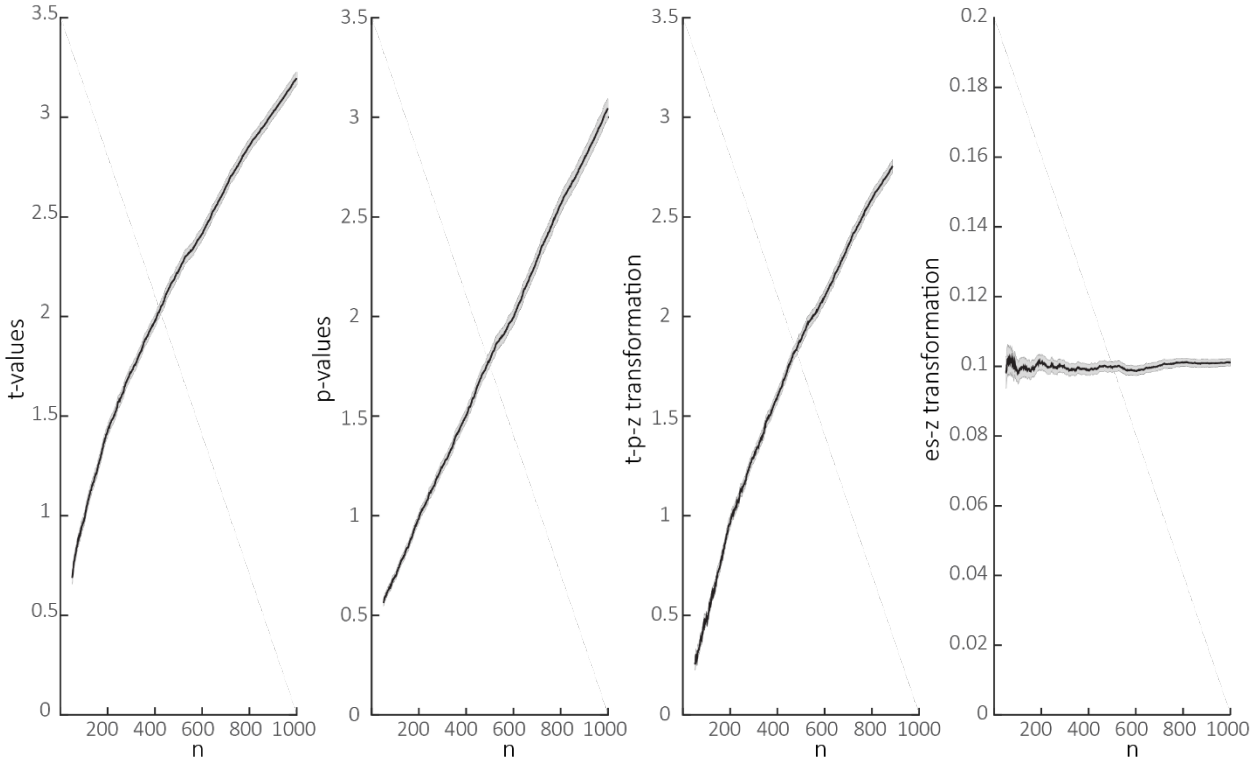

Figure 1: Effect of sample size on p, t and z values. We drew a vector of 1000 numbers from a mu=0.2 and s=1 random normal distribution to simulate an effect size of d=0.2, and calculated the p, t and z value of a t-test comparing the first n of these numbers against zero, varying n from 50 to 1000. The t-p-z values were calculated by performing the normal inverse of the Student's t cumulative distribution function. The es-z values were calculated as t/√(n-1). The graphs plot the mean±sem (over the 1000 simulations) of these values as a function of the number of samples (n) considered. For p, the values are plotted on a -log10 scale. Note how for a given effect size (cohen d=0.2) increasing sample size increases p, t, t-p-z values, while es-z values remain stable at a z-value equal to the simulated effect size.

2. Methods

Subjects, Task and Acquisition: Data were acquired from 24 healthy volunteers (two were excluded due to missing data or technical errors, N=22), on a 3T Philips scanner, using a commercial version of Philips' MB implementation (based on software release version R5.4). A 32-channel head coil was used. Functional data were acquired using different acquisition sequences (see table1). Two types of stimuli were used: Complex actions (CA) showed the hand interacting with the object in typical, goal directed actions. For example, the hand of the actor reached for the lighter placed on the table, grasped it, and lit the candle with it. Complex controls (CC) stimuli had the exact same setting as the CA but the actor's hand did not interact with or manipulate the object on the table, instead, made aimless hand movements. A block was composed of three movies of the same category (CA or CC) and lasted 7s. Each fMRI session was composed of 13 blocks per stimulus category for a total of 26 blocks, presented in a randomized order. The inter-block-interval lasted between 8 – 12 s and consisted of a fixation cross on a gray and blue background similar to the stimuli background. These sessions were presented to each subject multiple times, showing the same blocks but in different order, with each session acquired with a different acquisition sequence, varying in MB factor (table 1). The order of acquisition was randomized between subjects. Importantly, the duration of the sessions was similar (~8 min), but more functional volumes were acquired during

sessions at lower TRs. Two additional sequences were acquired (a 3x3x3.3mm, and a 2.7mm isotropic sequence with MB4 but SENSE 1.5), but these sequences are not relevant for the issue we discuss here and therefore not presented (for details about those see Bhandari et al., 2019).

Table 1. Parameters used for scanning.

Parameters	TR	2.45s	1.22s	0.63s
Multiband factor (MB)		1	2	4
SENSE acceleration factor (S)		2	2	2
Acquired voxel size (mm)		2.7 isotropic	2.7 isotropic	2.7 isotropic
Flip angle in degrees		79	64	50
Number of slices		44	44	44
Acquired volumes		200	400	780
Slice gap (mm)		0.27	0.27	0.27
Field of view (mm)		216x216x130.4	216x216x130.4	216x216x130.4

Preprocessing: Data were preprocessed using SPM12 (Wellcome Trust Centre for Neuroimaging, UCL, UK) with Matlab version 8.4 (The MathWorks Inc., Natick, USA). Briefly, functional images were slice-time corrected and then realigned to the estimated average. Anatomical images were co-registered to the mean functional image, and segmented. The normalization parameters that were generated during segmentation were used to bring all the images to the MNI space. The resampled voxel size for the functional images was 2 × 2 × 2 mm and 1 x 1 x 1 for the anatomical scans.

Subject-level GLM: Subject level GLM included CA and CC as two separate task predictors with each predictor having 13 blocks of 7s. Regressors included the six motion parameters estimated during realignment, first five principal components of cerebrospinal fluid and five principal components of white matter (total 16 regressors). As by default, the GLM involves a global normalization step, described in the SPM manual (https://www.fil.ion.ucl.ac.uk/spm/doc/spm12_manual.pdf), section 8.7 as "SPM computes the grand mean value $g_s = \sum_{n=1}^{N} \frac{g_{ns}}{N}$. This is the fMRI signal averaged over all voxels within the brain and all time points within session s. SPM then implements 'Session-specific grand mean scaling' by multiplying each fMRI data point in session s by $100/g_s$.". The model included a low-pass filter at 128s and autoregressive correction was performed using the FAST option (Bollmann, Puckett, Cunnington, & Barth, 2018; Todd et al., 2016). The t- contrast of interest was always CA-CC which activates the Action observation network (AON, Gazzola & Keysers, 2009, Figure 4B).

To further explore the effect of the sampling, we performed two additional subject-level ANOVAs, one for sequence with MB factor 2 and one for MB factor 4, where we decimated the data to include only the odd data points for MB2 and every 4th data point in MB4 sequence. This resulted in inclusion of 200 data points for MB2 and 195 data points for MB4 sequence. In the SPM model design, the TR was changed to 1.22*2 and 0.63*4 and the microtime resolution was changed from the default of 16 to 16*2 and 16*4 for MB2 and MB4 sequences respectively. All the other settings were same as described above.

Z transformations: For each subject, two z-transformations were applied to the SPM t-maps of the CA-CC contrast. For the t-p-z transformation, SPM t-maps were converted into z-maps using the normal inversion of the student's t - cumulative density. The z-values for higher t-value (~ t = 5.2) were estimated as infinite

using the above function. These z-values were assigned to be 9. For the es-z transformation z-maps were generated by reading out the degrees of freedom estimated by SPM while visualizing the CA-CC contrast, and then using the formula z=t/√(df).

Group-level GLM: To identify the effect of MB acceleration on voxel-wise, subject-level statistics, two within-subject group-level ANOVAs were performed, one with each type of z-transformation. Z maps were entered for the three sequences. Six pairwise contrasts were computed between the three sequences (MB1>MB2, MB1>MB4, MB2>MB4, MB2>MB1, MB4>MB1, MB4>MB2). All the results were evaluated at $q_{fdr}<0.05$ and $p_{uncorr}<0.01$ and cluster threshold of 50 voxels.
Two additional within-subject ANOVAs for the full vs. decimated dataset were also computed separately for MB2 and MB4 sequences. Full>decimated and decimated>full contrasts were computed. All the results were evaluated at $q_{fdr}<0.05$ and cluster threshold of 50 voxels.

To better understand the source of improvement in group level statics with MB (as reported in Bhandari et al., 2019), we subtracted the t-p-z-maps of MB1 from the t-p-z maps of MB2 and MB4 within the AON (18360 voxels) and another non-task network (18309 voxels) of similar size (see Figure 4B). The overlap between the two networks is minimal (70 voxels). The cumulative t-p-z values across all subjects were plotted for the two networks to see if we find a skewed distribution that would provide evidence that the benefit of MB acceleration is small and non-significant but may add up to show benefits at group level.

3. Results

For the t-p-z transformation, the pairwise contrasts between MBs showed no significant results at $q_{FDR}<0.05$. However, lowering the threshold to $p_{uncorrected}<0.01$ showed that within the AON, MB4 showed higher z values compared to MB1 and MB2 (see Figure 2, rows 1-3). There were 1640 voxels for the MB4-MB1 and 523 voxels for MB4-MB2 contrasts within the AON with higher z-values. The opposite contrast (i.e. MB1-MB4 and MB2-MB4) showed no significant voxels within the AON. This shows that while nothing survives after correcting for multiple comparisons, at a lower threshold, sequences with MB4 do show signs of better performance. The difference between MB1 and MB2 was not as well defined and within the AON, MB1 performed slightly better with 66 voxels showing better z-values for MB1-MB2 where as the MB2-MB1 contrast did not show any clusters in the AON.
For the es-z transformation, the contrast MB1-MB4 showed five clusters (452 voxels) within the AON that were significant at $q_{fdr}<0.05$ suggesting that the sequences without MB may perform slightly better. There were no other significant clusters outside the AON. Lowering the threshold to $p_{uncorrected}<0.01$ showed the similar trend where lower MBs performed better than the higher ones with more significant voxels within the AON (see Figure 2, rows 4-6). While MB2>MB1, MB4>MB1 and MB4>MB2 showed no significant clusters within the AON, MB1>MB2, MB1>MB4 and MB2>MB4 showed 1164, 4063 and 857 voxels respectively within the AON.

T-P-Z transformation

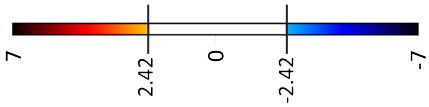

MB2-MB1

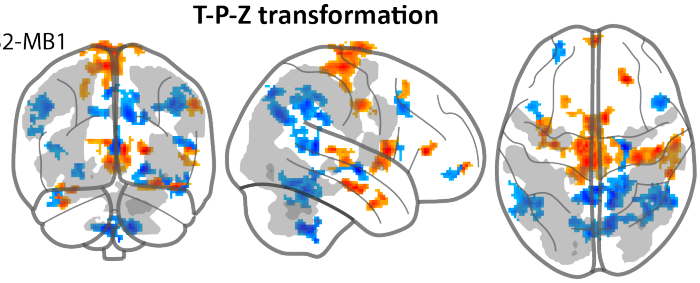

	total activated	overlap with AON
MB2>MB1	2104	0
MB1>MB2	2146	66

MB4-MB1

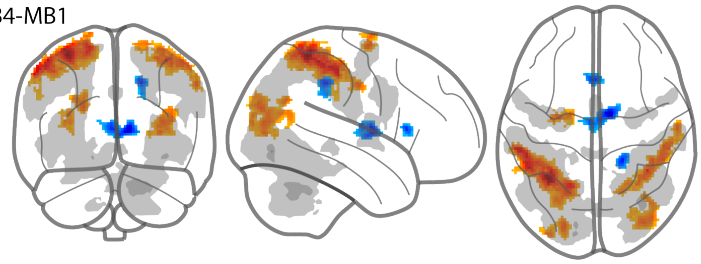

	total activated	overlap with AON
MB4>MB1	2597	1640
MB1>MB4	402	0

MB4-MB2

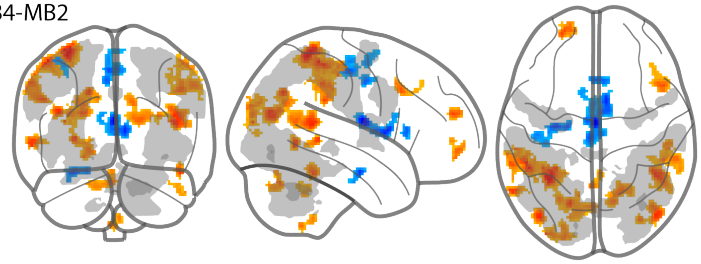

	total activated	overlap with AON
MB4>MB2	2816	523
MB2>MB4	798	0

es-Z transformation

MB2-MB1

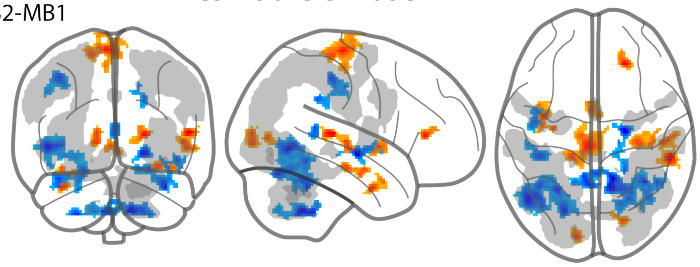

	total activated	overlap with AON
MB2>MB1	1300	0
MB1>MB2	2103	1164

MB4-MB1

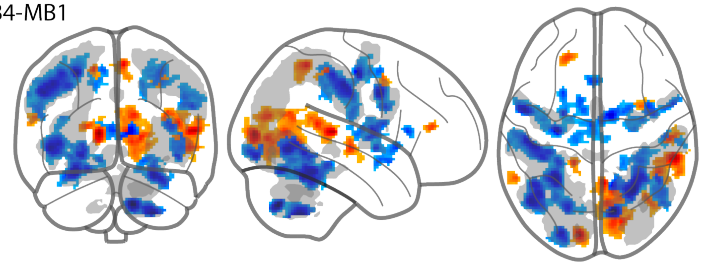

	total activated	overlap with AON
MB4>MB1	2729	0
MB1>MB4	5544	4063

MB4-MB2

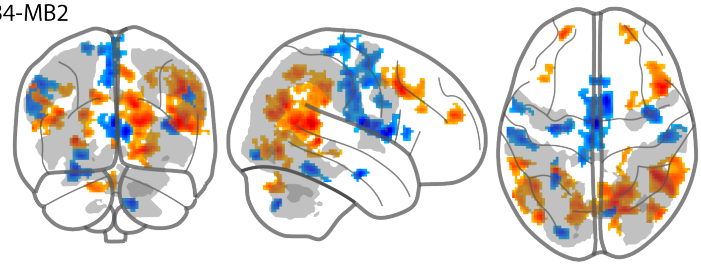

	total activated	overlap with AON
MB4>MB2	4332	0
MB2>MB4	2352	857

Figure 2: Pairwise contrasts between the three sequences. Row 1-3 for the t-p-z transformations and 4-6 for es-z transformations. Hot colours represent higher MB-lower MB and the cold colours are the opposite contrast. All the contrasts are evaluated at $p_{uncorrected}$<0.01 and a cluster threshold of 50 voxels. In grey are the areas that belong to the CA-CC network. It is derived from the group analysis of the same subjects but the data was acquires using a standard sequence with no MB and bigger voxel size (3x3x3.3mm) at q_{fdr}<0.05.

These contradicting results from different z-transformations require further analysis to understand which of the two transformations reflect the truth. However, since different sequences differ in more aspects (such as tSNR and grey white matter CNR) than in just the sampling rate, we analysed the decimated dataset against the full dataset for MB2 and MB4 sequences to see how number of samples alone affect the results. Since all the other image aspects are identical in full vs decimated data, we expected the full data to show better results than the decimated data due to the higher number of time points in the full data. For the t-p-z transformation we found no significant differences between the full and decimated versions of MB2 and MB4 data at q_{FDR}<0.05. Surprisingly, for the es-z transformation, for both MB2 and MB4 sequences, the decimated data performed significantly better than the full data at q_{FDR}<0.05 (Figure 3). This suggests that the es-z transformation penalizes the sequences with more samples and cannot be used as an objective measure to compare different MB sequences.

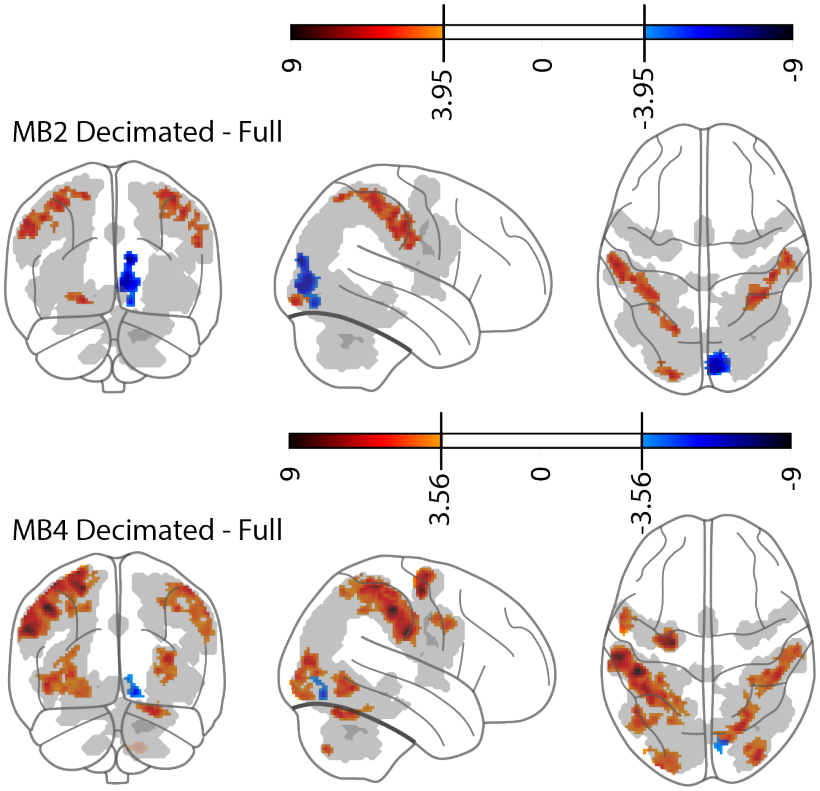

Figure 3: Pairwise contrasts [full>decimated/decimated>full] for MB2 and MB4 sequences. All the contrasts are evaluated at q_{fdr}<0.05 and a cluster threshold of 50 voxels.

To get a better idea about which sequence would 'win' for task-based fMRI, we plotted the cumulative (over subjects) t-p-zMB4 *minus* t-p-zMB1 histogram within the AON and within another non-task related network (Figure 4B). Figure 4A presents these histograms. While comparing the histogram (in blue) to its mirror (in orange), it is clear that for MB4 that the data is slightly positively skewed for the voxels in AON (pointed by the arrow) but not for the non-task network. This is not true for MB2 sequence. This confirms that going from MB1 to MB4, one can expect slightly higher z values in the network of interest for sequences with MB acceleration, but they are not enough to improve the subject level statistics, but potentially improves the group level results.

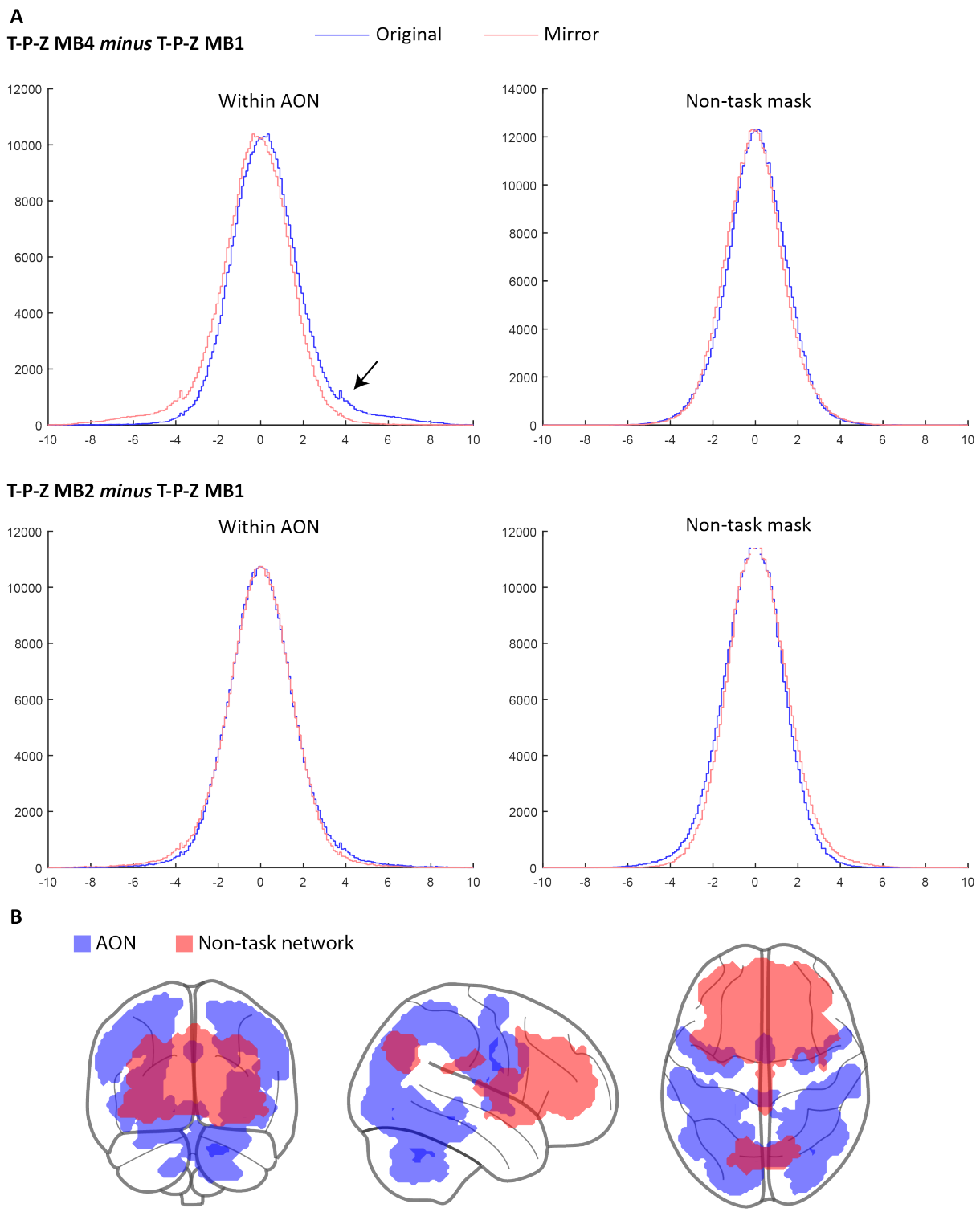

Figure 4. (a) Cumulative plots across subjects separately for t-p-z map for MB2-MB1 and MB4-MB1 within CA-CC mask and within another network mask of similar size. In blue are the original histogram and in orange is the mirror of the same to aid the visualization of the skewness. MB2-MB1 does not show skewness for any of the networks, but MB4-MB 1 shows a small deviation from normality (see black arrow) for the task network but not the other network where we do not expect any change. (b) Blue shows the task network (18360 voxels) and in pink is a network of similar size (18309 voxels). The overlap between these two networks is minimal (70 voxels).

4. Discussion

This is the first study that directly compares voxel-wise statistics between different sequences with varying acceleration achieved using MB technology to show that for task based studies, there is no significant advantage of MB in improving single subject level statistics. However, going from MB1 to MB4 we see small non-significant improvements in individual subject statistics which then potentially lead to improvement at group level. Our study is in line with other studies that use summary statistics with task based fMRI to show that the results of MB acceleration are comparable or slightly better (Boubela, Kalcher, Nasel, & Moser, 2014; Boyacioğlu et al., 2015; Moeller et al., 2010).

Directly comparing data coming from two sequences is not straightforward. Using the parameter estimates (Beta and con) for direct voxel-wise comparison of sequences with and without MB acceleration is not recommended, as the CNR is higher with longer TR leading to TR dependent scaling (Bhandari et al., 2019). This is due to the fact that global mean scaling, which is a default setting in SPM to bring the time series from subjects and groups to a common scale creates systematic biases when the CNR differs between conditions, and therefore makes the interpretation of results tricky. T-statistics should not be compared directly either, as for the same amount of acquisition time, many more samples are acquired for MB accelerated sequences, which results in higher degrees of freedom and therefore higher t-values, and higher critical t-values (i.e. the t-value above which a result is significant).

Z-transformation of the t-statistics appears to be a logical way to enable a direct comparison of two sequences with different TRs (with different numbers of acquired voxels) in terms of signal to noise ratio for detecting functional activations. A common way of transforming t-statistics is using the normal inverse of the student's t cumulative density. This form of z-transformation maps the p value of a GLM onto a normal distribution, but remains a metric of significance, which should increase with higher statistical power.

We also compared another way of transforming the data which is performed by dividing the t-values with the square root of the degrees of freedom. However, we found this transformation not to be a suitable as it penalized the data with higher degrees of freedom, leading to results that showed that sequences with no MB perform better than the sequences with MB. Since the tSNR decreases with increasing acceleration, this could be a valid result. However, when we decimated the data coming from MB2 and MB4 sequences, we found that the decimated sequences gave higher z values as compared to the full data set. Since the decimated data only differed in the number of samples and all the other image parameters are the same, the z values can either remain unchanged (if no additional information is added by the extra data points) or can increase due to the higher statistical power. This provides a clear evidence for the fact that this method of z-transformation is not appropriate while comparing sequences with different sampling rate.

This study have several weakness and strengths. While t-p-z conversion seems an appropriate way of comparing different sequences, the t values higher than ~5.2 are assigned as infinite. We then replace those values with a 'high' z-value of 9. This scenario is not ideal and may have a small impact on the results. However, this is the first study to combine the a large enough sample size (N=22), use of a cognitive task that activates a large network of brain regions and uses a stringent contrast to provide a direct comparison of different sequences, showing that at single-subject voxel-wise level, MB offers limited benefits for task based fMRI. However, these small advantages at single subject level potentially translate into small but significant improvements at group level.

Acknowledgements: This work was supported by the Netherlands Organization for Scientific Research (VIDI: 452-14-015 to V.G.), the Brain and Behavior Research Foundation (NARSAD young investigator 22453 to V.G.), the European Research Council of the European Commission (ERC-StG-312511 to C.K.) and the BIAL foundation grant (503 323 055 to V.G., C.K. & R.B.). We thank Spinoza centre for neuroimaging where the scanning was performed and the staff members of Spinoza centre.

Conflict of Interest: The authors report that there is no conflict of interest.

References:

Bhandari, R., Kirilina, E., Caan, M., Suttrup, J., de Sanctis, T., de Angelis, L., … Gazzola, V. (2019). Does higher sampling rate (Multiband + SENSE) benefit the detection of task correlated BOLD for cognitive neuroscience applications at 3T? *BioRxiv*. https://doi.org/10.1101/762831

Bollmann, S., Puckett, A. M., Cunnington, R., & Barth, M. (2018). Serial correlations in single-subject fMRI with sub-second TR. *NeuroImage*, *166*(Supplement C), 152–166. https://doi.org/https://doi.org/10.1016/j.neuroimage.2017.10.043

Boubela, R. N., Kalcher, K., Nasel, C., & Moser, E. (2014). Scanning fast and slow: current limitations of 3 Tesla functional MRI and future potential. *Frontiers in Physics*, *2*, 1. https://doi.org/10.3389/fphy.2014.00001

Boyacioğlu, R., Schulz, J., Koopmans, P. J., Barth, M., & Norris, D. G. (2015). Improved sensitivity and specificity for resting state and task fMRI with multiband multi-echo EPI compared to multi-echo EPI at 7 T. *NeuroImage*, *119*, 352–361. https://doi.org/http://dx.doi.org/10.1016/j.neuroimage.2015.06.089

Chen, L., Vu, A., Xu, J., Moeller, S., Ugurbil, K., Yacoub, E., & Feinberg, D. A. (2015). Evaluation of Highly Accelerated Simultaneous Multi-Slice EPI for FMRI. *NeuroImage*, *104*, 452–459. https://doi.org/10.1016/j.neuroimage.2014.10.027

Demetriou, L., Kowalczyk, O. S., Tyson, G., Bello, T., Newbould, R. D., & Wall, M. B. (2018). A comprehensive evaluation of increasing temporal resolution with multiband-accelerated protocols and effects on statistical outcome measures in fMRI. *NeuroImage*, *176*, 404–416. https://doi.org/https://doi.org/10.1016/j.neuroimage.2018.05.011

Feinberg, D. A., Moeller, S., Smith, S. M., Auerbach, E., Ramanna, S., Glasser, M. F., … Yacoub, E. (2010). Multiplexed Echo Planar Imaging for Sub-Second Whole Brain FMRI and Fast Diffusion Imaging. *PLoS ONE*, *5*(12), e15710. https://doi.org/10.1371/journal.pone.0015710

Gazzola, V., & Keysers, C. (2009). The Observation and Execution of Actions Share Motor and Somatosensory Voxels in all Tested Subjects: Single-Subject Analyses of Unsmoothed fMRI Data. *Cerebral Cortex (New York, NY)*, *19*(6), 1239–1255. https://doi.org/10.1093/cercor/bhn181

Griffanti, L., Salimi-Khorshidi, G., Beckmann, C. F., Auerbach, E. J., Douaud, G., Sexton, C. E., … Smith, S. M. (2014). ICA-based artefact and accelerated fMRI acquisition for improved Resting State Network imaging. *NeuroImage*, *95*, 232–247. https://doi.org/10.1016/j.neuroimage.2014.03.034

Kiss, M., Hermann, P., Vidnyánszky, Z., & Gál, V. (2018). Reducing task-based fMRI scanning time using simultaneous multislice echo planar imaging. *Neuroradiology*, *60*(3), 293–302. https://doi.org/10.1007/s00234-017-1962-4

Koopmans, P. J., Boyacioğlu, R., Barth, M., & Norris, D. G. (2012). Whole brain, high resolution spin-echo resting state fMRI using PINS multiplexing at 7 T. *NeuroImage*, *62*(3), 1939–1946. https://doi.org/http://dx.doi.org/10.1016/j.neuroimage.2012.05.080

Lindquist, M. A., & Mejia, A. (2015). Zen and the art of multiple comparisons. *Psychosomatic Medicine*, *77*(2), 114–125. https://doi.org/10.1097/PSY.0000000000000148

McDowell, A. R., & Carmichael, D. W. (2018). Optimal repetition time reduction for single subject event-related functional magnetic resonance imaging. *Magnetic Resonance in Medicine*, *0*(0). https://doi.org/10.1002/mrm.27498

Moeller, S., Yacoub, E., Olman, C. A., Auerbach, E., Strupp, J., Harel, N., & Uğurbil, K. (2010). Multiband Multislice GE-EPI at 7 Tesla, With 16-Fold Acceleration Using Partial Parallel Imaging With Application to High Spatial and Temporal Whole-Brain FMRI. *Magnetic Resonance in Medicine : Official Journal of the Society of Magnetic Resonance in Medicine / Society of Magnetic Resonance in Medicine*, *63*(5), 1144–1153. https://doi.org/10.1002/mrm.22361

Nadkarni, T. N., Andreoli, M. J., Nair, V. A., Yin, P., Young, B. M., Kundu, B., … Prabhakaran, V. (2014). Usage of fMRI for pre-surgical planning in brain tumor and vascular lesion patients: task and statistical threshold effects on language lateralization. *NeuroImage. Clinical*, *7*, 415–423. https://doi.org/10.1016/j.nicl.2014.12.014

Ni, B., Wang, X., Yu, T., Wu, R., & Wang, B. (2019). Pre-surgical Language Mapping in Epilepsy: Using fMRI in Chinese-Speaking Patients. *Frontiers in Human Neuroscience*, *13*, 183. https://doi.org/10.3389/fnhum.2019.00183

Preibisch, C., Castrillón G., J. G., Bührer, M., & Riedl, V. (2015). Evaluation of Multiband EPI Acquisitions for Resting State fMRI. *PLoS ONE*, *10*(9), e0136961. https://doi.org/10.1371/journal.pone.0136961

Sahib, A. K., Erb, M., Marquetand, J., Martin, P., Elshahabi, A., Klamer, S., … Focke, N. K. (2018). Evaluating the impact of fast-fMRI on dynamic functional connectivity in an event-based paradigm. *PLoS ONE*, *13*(1), e0190480. https://doi.org/10.1371/journal.pone.0190480

Sahib, A. K., Mathiak, K., Erb, M., Elshahabi, A., Klamer, S., Scheffler, K., … Ethofer, T. (2016). Effect of temporal resolution and serial autocorrelations in event-related functional MRI. *Magnetic Resonance in Medicine*, *76*(6), 1805–1813. https://doi.org/10.1002/mrm.26073

Todd, N., Josephs, O., Zeidman, P., Flandin, G., Moeller, S., & Weiskopf, N. (2017). Functional Sensitivity of 2D Simultaneous Multi-Slice Echo-Planar Imaging: Effects of Acceleration on g-factor and Physiological Noise . *Frontiers in Neuroscience* . Retrieved from https://www.frontiersin.org/article/10.3389/fnins.2017.00158

Todd, N., Moeller, S., Auerbach, E. J., Yacoub, E., Flandin, G., & Weiskopf, N. (2016). Evaluation of 2D multiband EPI imaging for high-resolution, whole-brain, task-based fMRI studies at 3T: Sensitivity and slice leakage artifacts. *Neuroimage*, *124*(Pt A), 32–42. https://doi.org/10.1016/j.neuroimage.2015.08.056

Wengenroth, M., Blatow, M., Guenther, J., Akbar, M., Tronnier, V. M., & Stippich, C. (2011). Diagnostic benefits of presurgical fMRI in patients with brain tumours in the primary sensorimotor cortex. *European Radiology*, *21*(7), 1517–1525. https://doi.org/10.1007/s00330-011-2067-9